胎生期マウス舌発生過程における Nfix を介した筋分化制御

川本沙也華

Nuclear factor 1 X-type-associated regulation of myogenesis in developing mouse tongue

Sayaka KAWAMOTO

日本歯科大学大学院生命歯学研究科歯科基礎系専攻
（指導：添野雄一 教授）

研究指導：田谷雄二 准教授
（日本歯科大学生命歯学部病理学講座）

The Nippon Dental University, Graduate School of Life Dentistry at Tokyo
(Supervisor: Prof. Yuuichi SOENO)

Directed by
Associate Prof. Yuji TAYA
The Nippon Dental University, Graduate School of Life Dentistry at Tokyo,
Department of Pathology

（2023 年 2 月）

この論文の内容は次の形式で公表した。

論文題名： Nuclear factor 1 X-type-associated regulation of myogenesis in developing mouse tongue

雑 誌 名： Journal of Oral Biosciences (accepted)

著 者 名： Sayaka KAWAMOTO, Taisuke HANI, Kazuya FUJITA, Yuji TAYA, Yasunori SASAKI, Tomoo KUDO, Kaori SATO and Yuuichi SOENO

この論文を川本沙也華の博士（歯学）学位論文として提出することを承諾します。

添野　雄一　　印

田谷　雄二　　印

佐藤　かおり　　印

工藤　朝雄　　印

本研究は日本学術振興科学研究費補助（JP23792116, JP15K11024, JP18K09530, JP21K09822)を受けて行われた。

Contents

Abstract

Objectives: The tongue contains skeletal myofibers that differ from those in the trunk, limbs, and other orofacial muscles. However, the molecular basis of myogenic differentiation in the tongue muscles remains unclear. In this study, we conducted comprehensive gene expression profiling of the developing murine tongue.

Methods: Tongue primordia were dissected from mouse embryos at embryonic day (E)10.5–E18.5, while myogenic markers were detected via microarray analysis and quantitative polymerase chain reaction (PCR). In addition to common myogenic regulatory factors such as *Myf5*, *MyoD*, *myogenin*, and *Mrf4*, we focused on *Nfix*, which acts as a unique molecular switch triggering the shift from embryonic to fetal myoblast lineage during limb myogenesis. *Nfix* inhibition was performed using a specific antisense oligonucleotide in the organ culture of tongue primordia.

Results: Microarray and ingenuity pathway analyses confirmed the significant upregulation of myogenic signaling molecules, including *Nfix*, associated with the differentiation of myoblasts from myogenic progenitor cells during E10.5–E11.5. Quantitative PCR confirmed that *Nfix* expression started at E10.5 and peaked at E14.5. Fetal myoblast-specific genes, such as *Mck* and *Myh8*, were upregulated after E14.5, whereas embryonic myoblast-specific genes, such as *Myh3* and *Myh7*, were downregulated. When *Nfix* was inhibited in the organ culture of tongue primordia, subtle morphological differences were noted in the tongue. Such an observation was only noted in the cultures of E10.5-derived tongue primordia.

Conclusions: These results reveal the contribution of *Nfix* to tongue myogenesis. *Nfix* expression during early tongue development may play a vital role in tongue muscle development.

1. Introduction

In skeletal myogenesis, muscle precursor cells that express the paired box genes Pax3 and Pax7 are committed to becoming myogenic cells. They differentiate into myoblasts, fuse to form myotubes, and then develop into mature myofibers [1–4]. The determination and terminal differentiation of muscle cells are governed precisely by a signaling network with four muscle-specific transcription factors known as myogenic regulatory factors (MRFs): Myf5, MyoD, myogenin, and Mrf4 [5–9]. MRF signaling is supported by cofactors such as myocyte enhancer factor 2 (Mef2) and epigenetic modulators such as a panel of muscle-specific microRNAs known as "myomiRs" [3,10].

During skeletal myogenesis in mice, stage-specific transcriptional changes occur in muscle fibers derived from two discrete myogenic cells, namely, embryonic and fetal myoblasts [11–14]. Embryonic myoblasts form primary fibers between embryonic day (E)10.5 and E12.5, which establishes the basic muscle pattern (embryonic myogenesis). The second wave of myogenesis (fetal myogenesis) occurs between E14.5 and E17.5, which involves the fusion of fetal myoblasts either with each other to form secondary fibers that surround primary fibers or with primary fibers [15].

The tongue contains skeletal myofibers, but they differ from the myofibers found in the trunk, limbs, and other orofacial muscles with respect to the origin of myogenic precursor cells [16–18]. Previous studies on tongue morphogenesis emphasized the molecular basis of tongue myogenesis in tissue–tissue interactions between myogenic precursor cells and cranial neural crest cells (CNCC) [19,20]. Compared with the myogenesis of other skeletal muscles, myogenesis of tongue muscles involves the preferential expression of *Myf5* rather than *MyoD* during myoblast differentiation [21,22]. In addition, the characterization of embryonic, fetal, and neonatal tongue myoblasts *in vitro* demonstrated that lineage differences did not exist at the level of MRF expression but at the level of contractile genes such as those encoding myosin heavy chains (MyHCs) [23]. At present, this finding indicates that limb and tongue muscles share factors implicated in initial processes such as myogenic specification and migration, whereas factors for myogenic determination, differentiation, and maturation in tongue muscles remain unclear [20,24].

Nuclear factor 1 X-type (Nfix) is a transcription factor that can be used to determine myogenic cell fate because of its role as a differentiation switch triggering the shift from embryonic to fetal myoblast lineages (Fig.1A) [25,26]. The nuclear factor 1 (Nfi) family consists of four closely related genes, namely, *Nfia*, *Nfib*, *Nfic*, and *Nfix* in amniotes [27]. Nfi-binding sites are present on the myogenin promoter, and Nfi can form a complex with myogenin [28,29]. Thus, Nfi may play a role in the regulation of certain muscle-specific genes. The phenotypes in *Nfix* knockout mice display skeletal muscle abnormalities as well as bone and brain malformations [30]. *Nfix* has also been linked to muscular dystrophy, and its silencing or overexpression in postnatal dystrophic mice affected the disease state [31]. Genome-wide expression analysis on limb-derived embryonic and fetal myoblasts revealed that *Nfix* was highly expressed in the fetus but not in the embryo [32]. However, contrary to well-studied limb myogenesis, little is known about the *Nfix*-associated molecular basis of tongue myogenesis.

In this study, we performed comprehensive gene expression profiling of mouse tongue myogenic cells, particularly focusing on myoblast differentiation and *Nfix*-mediated regulation of myogenic signaling.

2. Materials & Methods

2.1. Animal maintenance

Female timed-pregnant ICR mice were purchased from a local supplier (Charles River Inc., Kanagawa, Japan). All mice were maintained under a 12-h light–dark cycle at 22°C and provided standard laboratory fodder and water *ad libitum*. For each dam, the morning of the day on which a vaginal plug was found was designated as E0.5. On each of the subsequent embryonic days—E10.5, E11.5, E.12.5, E13.5, E14.5, E16.5, and E18.5—dams were euthanized by cervical dislocation. Their uteri were excised and placed in Hank's balanced salt solution (HBSS; Thermo Fisher Scientific, Waltham, MA, USA) at 4°C. Embryos were rinsed with fresh HBSS to remove amniotic fluid and blood and were dissected to remove the primordium of the tongue under a stereomicroscope. For histological analysis, dissected tongue tissues were fixed with formalin and embedded in paraffin blocks.

2.2. Isolation of RNA from tongue primordia

For gene expression analysis of the sequence of tongue development, the medial part of the fused mandibular prominences that corresponds to a tongue primordium at E10.5 and E11.5 and the anterior two thirds of the tongue at the E12.5, E13.5, E14.5, E16.5, and E18.5 stages were collected (Fig. 1B). Total RNA was extracted from the tongue primordia that were dissected at each developmental stage using an RNA mini-kit (QIAGEN, Hilden, Germany) according to the manufacturer's instructions. The quality of RNA in the solutions was assessed using the Agilent Bioanalyzer (Agilent, Santa Clara, CA, USA). The concentration of the purified RNA was measured using the Nanodrop ND-1000 spectrophotometer (Thermo Fisher Scientific). The RNA fractions obtained in this study exhibited absorbance ratios at A260/A280 and A260/A230 of at least 1.8 and 2.0, respectively.

2.3. Microarray and signaling pathway analyses

We focused on the critical stages of tongue myogenesis, namely, E10.5 (settlement of myogenic progenitors in tongue primordium), E11.5 (initiation of myoblast differentiation with the development of lateral lingual swellings), and E14.5 (myoblast maturation and myofiber formation). The tongue primordia were collected from approximately 40 embryos per stage to obtain sufficient total RNA for microarray analysis (>3 μg). Microarray and statistical analyses were performed at the core facility of Cell Innovator Inc. (Fukuoka, Japan). In brief, a GeneChip Mouse Genome 430 2.0 array (Affymetrix, Santa Clara, USA) was hybridized with cRNA probes. The expression value and detection calls were computed from the raw data following the procedures outlined in Affymetrix MAS5.0. The normalized data were subjected to Student's t-test ($P < 0.05$) and were required to have a median fold change of ≥5 for selection. In addition, the microarray data were deposited in the Gene Expression Omnibus database (accession #GSE35091). Signaling pathways relevant to myogenesis were predicted using Ingenuity® Pathway Analysis (IPA, QIAGEN).

2.4. Real-time qPCR for mRNAs

The RNA isolated from tongue primordia at each developmental stage was used. cDNA was synthesized using an oligo-dT primer and the SuperScript® First-strand synthesis system for RT-PCR (Thermo Fisher Scientific). qPCR was performed using the SYBR Green I® PCR Master Mix (Thermo Fisher Scientific) and Prism 7000 Real-time PCR System (Thermo Fisher Scientific). The primer sets used in this study are listed in Table S1. All samples were assayed in triplicate. The cycle threshold (Ct) value of each target gene was normalized relative to an internal control (*GAPDH*) using the comparative ΔCt method.

2.5. Organ culture of tongue primordia and antisense oligonucleotide treatment

Trowell organ culture of mouse mandibular arches was performed as previously described [33]. In brief, the embryos at E10.5 were used to collect mandibular arches. Pairs of mandibular arches were positioned with the dorsal surface uppermost on a filter membrane, ensuring that the medial regions of the pair of mandibular arches were in close apposition. Subsequently, they were cultured for 48 and 96 h (37°C, 5% CO_2 in humidified air). The medium comprised Dulbecco's Modified Eagle Medium/Ham's Nutrient Mixture F12 Medium (1:1) containing Glutamax (Thermo Fisher Scientific) supplemented with 20% fetal bovine serum, 0.04 mg/mL ascorbate, and 1% penicillin/streptomycin. Cultured tissues were continuously treated with 10 nmol morpholino antisense oligonucleotides against *Nfix* mRNA or control (scrambled) oligonucleotides during culture. All oligonucleotides were commercially procured from Gene Tools LLC (Philomath, OR, USA). These oligonucleotides targeted specific regions in the 25-oligomer, including or near to the start codon of *Nfix* mRNA. The morpholino antisense oligonucleotide sequences were as follows: murine *Nfix*_5′-ACTCATCCATTGATCTGAAGCACCC-3′ and 5′-GGCAAAGCCAACGCCTGATTCTGAG-3′ and murine control sequence 5′-CCTCTTACCTCAGTTACAATTTATA-3′. These morpholinos are originally designed for *in vivo* use and therefore permeate well into cultured tissue. We preliminary checked the toxicity by comparing culture specimens with scrambled control oligonucleotides to those without oligonucleotides (no treatment) and confirmed that there were no histological differences.

2.6. Immunohistochemistry

Immunohistochemistry was performed on formalin-fixed paraffin-embedded tongue primordia sections (4-μm thickness) of E10.5–E11.5 embryos. The following antibodies were used: mouse anti-human desmin (DAKO, Japan), anti-mouse MyoD (SantaCruz Biotechnology, USA), and anti-human Nfix (LifeSpan BioSciences, USA). Antigens on the tissue sections were retrieved either by enzymatic digestion (0.1% pepsin for 10 min at 37°C or 0.002% proteinase K for 10 min at room temperature) or by microwave exposure in a buffer (10 mM citric acid [pH6.0]) for 10 min at 90°C (H2800, Energy Beam Sciences, USA). Immunocomplexes labeled with an Alexa-labeled secondary antibody (Alexa488/568) and DAPI-stained nuclei (SlowFade Antifade kit with DAPI, Invitrogen) were detected using a laser-scanning confocal microscope (Carl Zeiss, Germany).

2.7. Statistical analysis

Multiple comparison test (Tukey) was performed for time-series qPCR data. Since we presented the qPCR dataset as showing the chronological expression pattern of each gene, only the significant items that correspond to microarray datasets (E10.5–E11.5 and E11.5–E14.5) were indicated in the figures. Gene expression profiles in culture groups were assessed using Welch's t-test. All values are presented as mean ± standard deviation. *P* values of <0.05 were considered statistically significant.

3. Results

3.1. Histological features of developing mouse tongue

We firstly revisited the morphology of muscle cells in developing mouse tongue [34] (Fig. 2A). At the beginning of tongue morphogenesis, a pair of mandibular prominences faced each other at E9.5, fused at the midline at E10.5, and grew as lateral lingual swellings at E11.5. During this period, cells were assumed to be the hybrid population of occipital somite-derived myogenic progenitor cells, and CNCC were not discernible by their morphology. At E12.5, spindle-shaped cells emerged within the mesenchymal cell

population. Between E13.5 and E14.5, cells that were fused with neighboring cells were prominent and aligned alternately in a textile-like fashion. At E16.5 and beyond, muscle fibers were evident and the nuclei of the muscle cells were condensed. Besides the H–E-stained histology, immunostaining verified that assembled desmin-positive myogenic cells gradually adopted an elongated spindle-like shape along with tongue histogenesis (Fig. 2B).

3.2. Expression patterns of muscle-related genes during mouse tongue development

The expression pattern of individual MRF genes was determined via qPCR (Fig. 2C). Prior to the emergence of tongue primordium, no expression of the *Pax3* or MRF genes was detected in the medial region of mandibular prominences at E9.5 (data not shown). At E10.5, *Pax3*, *Myf5*, and *Myod1* (MyoD) were expressed in the tongue primordium. *Myog* (myogenin) and *Mrf4* (*Myf6*) were expressed from E11.5 and E12.5, respectively. The expression of these genes was maintained at various levels throughout the developmental period analyzed. *Mef2c* expression was gradually increased from E10.5 to E14.5, and the expression level was maintained thereafter.

3.3. Gene expression profiles and predicted molecular networks in tongue myogenesis

By cross-comparing the microarray datasets from E10.5 and E11.5 (designated as E10.5–E11.5), 102 genes that were differentially expressed by a >5-fold-change ($P < 0.05$) were identified. Of the 102 genes, 76 were upregulated and 26 were downregulated. Half of the upregulated genes were muscle-related genes, including MRFs, actins, and myosins (Table 1). Notably, *Nfix* was included in the upregulated gene group.

IPA of the differentially expressed genes revealed biological processes that might be activated during tongue development ($P < 0.05$; Table 2). In E10.5–E11.5, the top-ranking annotation “Development of muscle” indicated significant activation of muscle-related events during this period. However, the top-ranking annotation in E11.5–E14.5 was “Contractility of muscle,” which is linked to the functional features of myofibers. The predicted molecular networks that might function within the corresponding stages are listed in Table 3. In addition to MRF genes, several muscle-related transcriptional regulators, namely, *Mef2*, *Meox1*, *Meox2*, *Nkx2-5*, *Tcf21*, *Nfix*, and *Lbx1*, were

conspicuous in the three top-ranked networks in E10.5–E11.5. Conversely, the top-ranked networks in E11.5–E14.5 involved *Pax7*; however, no other muscle-related transcriptional regulators were predicted.

3.4. Expression of Nfix and related genes during embryonic–fetal myoblast transition

In addition to MRF gene expression profiling (Fig. 2C), the expression patterns of *Nfix* and other genes related to differentiation switch triggering the shift from embryonic myoblast to fetal myoblast lineage were evaluated by qPCR (Fig. 3A, 3B). Although changes in the expression level were not much drastic in qPCR (due to the efficiencies in primer annealing and amplification), all the genes upregulated in microarray were reproducibly upregulated in qPCR. Embryonic myoblast markers, namely, *Meox1* and *Meox2*, began to be expressed at E10.5, with their expression peaking at E11.5 and then gradually decreasing through the developmental period. Thereafter, the expression of *Myh3* and *Myh7* began at E11.5 and peaked at E13.5. Besides, the expression of *Nfix* started at E10.5 and peaked at E14.5, followed by stable expression at a lower level up to E18.5. The induction of *Eno3* increased after E14.5, which was the peak expression of *Nfix*. *Myh8*, a fetal/perinatal component of MyHCs, was also expressed from E11.5, with its expression increasing in parallel with that of *Nfix* and peaking at E14.5.

3.5. Appearance of Nfix protein-expressing myogenic cells in tongue primordia

Immunohistochemistry was used to confirm the expression of *Nfix* at the protein level in the embryonic and fetal myogenic stages (Fig. 4). In the tongue primordium at E11.5, the MyoD signal, which was used as a myoblast marker, was detected as a single nucleus within the desmin-positive cell population. On the other hand, dot-like Nfix signals were detected within the nuclei of desmin-positive myogenic cells, but such signals were weaker than MyoD signals. At E14.5, Nfix-expressing cells with intense signals were apparent in the nuclei of desmin-positive cells.

3.6. Impairment of myogenesis by the inhibition of Nfix transcript in vitro

For validating the Nfix function in tongue myogenesis, tongue primordia were collected from E10.5 embryos and subjected to organ culture either with the addition of

morpholino antisense oligonucleotides (*Nfix*-inhibited group) or with scrambled/control oligonucleotides (control group) into the culture medium (Fig. 5A). The morpholino oligos sterically inhibit mRNAs to be translated into functional proteins. In fact, Nfix protein expression was impaired in the *Nfix*-inhibited group after 48 h of culture. The expression level of *Nfix* transcript between the two experimental groups was, albeit showing a statistical difference, almost comparable (Fig. 6A). Based on histological observation (Fig. 5B), no evident abnormality in the formation of the tongue primordium was found after 48 h of culture. After 96 h, tongue morphogenesis resulted in the formation of a dense cell population; no difference in size and width of the formed tongue was observed between the two groups. Immunostaining of Ki-67 revealed active cell proliferation in the epithelium and mesenchyme. In addition, desmin immunostaining verified the localization of desmin-positive cells in the tongue. Notably, elongated/spindle-shaped desmin-positive cells emerged in the control group. Spindle-shaped desmin-positive cells were also found in the *Nfix*-inhibited group, but the cell length was relatively shorter than that in the control group. Moreover, a wide cell-free interspace was observed in the mesenchymal cell region underneath the epithelium only in the histological specimens of the *Nfix*-inhibited group cultured for 96 h. qPCR verified that the expression of *Nfix* and its downstream genes *Nfatc4* and *Eno3* was significantly affected, but practically comparable (Fig. 6B).

Furthermore, tongue primordia collected from E11.5 embryos were cultured for 48 and 96 h. Consequently, no difference was found in any parameter between the control and *Nfix*-inhibited groups; cell-free interspace was not observed, and cell shape was on a level (Fig. 6C).

4. Discussion

This study aimed to investigate the molecular basis of myoblast differentiation in tongue myogenesis, which remains unclear to date. Thus, we focused on *Nfix* as a leading modulator of tongue embryonic and fetal myoblast differentiation as established previously in limb myogenesis.

Limb skeletal muscles in mice are formed between E14.5 and E17.5 [15]. A previous

study analyzed the expression of genes in the tongue and hindlimbs of E11, 13, 15, and 17 mice and revealed that the expression of myogenic markers such as *desmin*, *Mck*, *troponin C*, and MRFs peaked in tongue muscles 2 days earlier than in hindlimb skeletal muscles, indicating that myoblast differentiation in the tongue is activated at E13–15 and progresses earlier than that in skeletal and masseter muscles [35]. To make this point clearer, we performed comparison analysis of gene expression profiles among tongue primordia at E10.5, E11.5, and E14.5. In consequence, microarray analysis revealed that not only MRFs but also other muscle-related transcriptional regulators were upregulated from E10.5 to E11.5. The dominancy of myogenic molecular networks is an intriguing finding since various tissues are growing concomitantly in this stage. In particular, we also found that embryonic and fetal myoblast markers (such as *Meox1*, *Meox2*, and *Nfix*) were upregulated. Indeed, qPCR analysis in time-series from E10.5 to E18.5 confirmed that these muscle-related genes were concurrently expressed in the early developmental stage of tongue primordia. These data indicated that myogenesis, including embryonic and fetal myoblast differentiation, progresses to tongue primordia development by as early as E10.5.

Notably, IPA-assisted prediction suggested that *Nfix* participates in a certain network that might be activated in E10.5–E11.5 (Table 3). qPCR validation also indicated that the expression of *Nfix* started at E10.5 and increased thereafter until E14.5. This is a valuable finding because fetal myogenesis occurs between E14.5 and E17.5 in the limb [11]; the activation of *Nfix* in tongue myogenesis is unlikely concurrent with that in limb myogenesis. In addition, the fetal myoblast marker *Eno3* was upregulated after the peak expression of *Nfix* at E14.5, while the expression of embryonic myoblast-specific *Myh7* decreased along with the downregulation of *Nfatc4*, a direct target of Nfix. The expression of *Myh8* (MyHC-perinatal gene) started from E11.5 and peaked at E14.5, which was similar to the expression of *Nfix*. This finding indicates the presence of *Myh8*-expressing myoblasts, at least from E11.5 onward, which is consistent with a previous finding in that myoblast obtained from mouse tongue at E12.0 expressed *Myh3* (MyHC-embryonic gene) and *Myh8* [23]. These findings support the involvement of *Nfix* in tongue muscular differentiation at a relatively early stage of tongue development.

The abovementioned microarray and qPCR results proposed that *Nfix* is a key

regulator indispensable to early differentiation of tongue myoblasts. Thus, the *Nfix* transcript in the organ culture system was impaired to verify this hypothesis. Although no remarkable difference was found in tongue morphogenesis between the *Nfix*-inhibited and control groups, some discernible differences were observed. Desmin-positive cells in the *Nfix*-inhibited group appeared less elongated than those in the control group. In addition, in all histological specimens of the *Nfix*-inhibited group, a wide cell-free interspace was found in the mesenchymal cell region underneath the epithelium. The cell-free interspace corresponds to the region where Ki-67-negative mesenchymal cells are localized in the control group. The cause of this empty space might be due to impaired cell-to-cell adhesion, but the initial trigger remains unclear. The inhibition of *Nfix* might affect the structural balance between the muscular–mesenchymal interface. Importantly, when tongue primordia collected from E11.5 embryos were cultured, no such differences were observed between the *Nfix*-inhibited and control groups. This indicates that *Nfix* expressed in E11.5 has minimal effect on tongue muscle differentiation, or rather, *Nfix* expressed in E10.5 can drive the early phase of tongue development.

Considering the importance of *Nfix* in inducing tongue myogenesis, it is still questionable why *Nfix* inhibition resulted in marginal impact on tongue development. Such questions might be related to the finding that the immunohistochemical detection of Nfix weakened with the increase in transcripts at E11.5. This finding might be partly due to the repression of the translation of the *Nfix* transcript by miRNAs. Among *Nfix*-targeting miRNAs predicted by the IPA platform, the expression levels of miR-152 and miR-378 were maintained at a substantial level throughout tongue development (Supplementary Fig. S1). This expression pattern was different from that of myomiRs, which increased with tongue myogenesis. Other studies have provided evidence for the multiple roles of these miRNAs in myogenic signaling pathways, for example, miR-378 was reported to repress *MyoR* (*Msc*), a repressor of *MyoD* [36]. These facts suggest that *Nfix*-targeting miRNA candidates, together with other cognate miRNAs, exert a profound effect on *Nfix*-mediated myoblast differentiation signaling, which is a future research topic.

5. Conclusions

The expression profile of *Nfix* and its related genes support the theory that *Nfix* plays a crucial role in tongue muscle development. Unlike in the limb, *Nfix*-mediated signaling proceeds from the beginning of tongue myogenesis, which might be indispensable to form the basis for the unique feature of lingual movement and function.

Ethical Approval

Animal maintenance and handling protocols were in compliance with the institutional approval (#32667) and followed the guidelines of the Animal Care and Use Committee of the Nippon Dental University.

Acknowledgments

We thank Edanz (https://jp.edanz.com/ac) for editing a draft of this manuscript. This work was supported by Grants-in-Aid for Scientific Research (JSPS KAKENHI Grant Numbers JP23792116 for KF., and JP15K11024, JP18K09530 and JP21K09822 for YT).

Conflicts of interest

The authors declare no potential conflicts of interest with respect to the authorship and/or publication of this article.

References

[1] Kassar-Duchossoy L, Giacone E, Gayraud-Morel B, Jory A, Gomès D, Tajbakhsh S. Pax3/Pax7 mark a novel population of primitive myogenic cells during development. Genes Dev 2005;19:1426–31.

[2] Relaix F, Montarras D, Zaffran S, Gayraud-Morel B, Rocancourt D, Tajbakhsh S, et al. Pax3 and Pax7 have distinct and overlapping functions in adult muscle progenitor cells. J Cell Biol 2006;172:91–102.

[3] Braun T, Gautel M. Transcriptional mechanisms regulating skeletal muscle differentiation, growth and homeostasis. Nat Rev Mol Cell Biol 2011;12:349–61.

[4] Chal J and Pourquié O. Making muscle: skeletal myogenesis *in vivo* and *in vitro*. Development 2017;144:2104–22.

[5] Hasty P, Bradley A, Morris JH, Edmondson DG, Venuti JM, Olson EN, et al. Muscle deficiency and neonatal death in mice with a targeted mutation in the myogenin gene. Nature 1993;364:501–6.

[6] Nabeshima Y, Hanaoka K, Hayasaka M, Esumi E, Li S, Nonaka I, et al. Myogenin gene disruption results in perinatal lethality because of severe muscle defect. Nature 1993;364:532–5.

[7] Pownall ME, Gustafsson MK, Emerson CPJr. Myogenic regulatory factors and the specification of muscle progenitors in vertebrate embryos. Annu Rev Cell Dev Biol 2002;18:747–83.

[8] Berkes CA, Tapscott SJ. MyoD and the transcriptional control of myogenesis. Semin Cell Dev Biol 2005;16:585–95.

[9] Hernández-Hernández JM, García-González EG, Brun CE, Rudnicki MA. The myogenic regulatory factors, determinants of muscle development, cell identity and regeneration. Semin Cell Dev Biol 2017;72:10–18.

[10] Mok GF, Lozano-Velasco E, Münsterberg A. microRNAs in skeletal muscle development. Semin Cell Dev Biol 2017;72:67–76.

[11] Tajbakhsh S. Skeletal muscle stem and progenitor cells: Reconciling genetics and lineage. Exp Cell Res 2005;306:364–72.

[12] Biressi S, Molinaro M, Cossu G. Cellular heterogeneity during vertebrate skeletal muscle development. Dev Biol 2007;308:281–93.

[13] Murphy M, Kardon G. Origin of vertebrate limb muscle: the role of progenitor and myoblast populations. Curr Top Dev Biol 2011;96:1–32.

[14] Esteves de Lima J, Relaix F. Master regulators of skeletal muscle lineage development and pluripotent stem cells differentiation. Cell Regen 2021;10:31. doi:10.1186/s13619-021-

00093-5.

[15] Messina G, Cossu G. The origin of embryonic and fetal myoblasts: a role of Pax3 and Pax7. Genes Dev 2009;23:902–5.

[16] Noden D. The embryonic origins of avian cephalic and cervical muscles and associated connective tissues. Am J Anat 1983;168:257–76.

[17] Huang R, Zhi Q, Izpisua-Belmonte JC, Christ B, Patel K. Origin and development of the avian tongue muscles. Anat Embryol (Berl) 1999;200:137–52.

[18] Yamane A. Embryonic and postnatal development of masticatory and tongue muscles. Cell Tissue Res 2005;322:183–9.

[19] Hosokawa R, Oka K, Yamaza T, Iwata J, Urata M, Xu X, et al. TGF-β mediated FGF10 signaling in cranial neural crest cells controls development of myogenic progenitor cells through tissue-tissue interactions during tongue morphogenesis. Dev Biol 2010;341:186–95.

[20] Parada C, Han D, Chai Y. Molecular and cellular regulatory mechanisms of tongue myogenesis. J Dent Res 2012;91:528–35.

[21] Rudnicki MA, Schnegelsberg PN, Stead RH, Braun T, Arnold HH, Jaenisch R. MyoD or Myf-5 is required for the formation of skeletal muscle. Cell 1993;75:1351–9.

[22] Dalrymple KR, Prigozy TP, Mayo M, Kedes L, Shuler CF. Murine tongue muscle displays a distinct developmental profile of MRF and contractile gene expression. Int J Dev Biol 1999;43:27–37.

[23] Dalrymple KR, Prigozy TI, Shuler CF. Embryonic, fetal, and neonatal tongue myoblasts exhibit molecular heterogeneity in vitro. Differentiation 2000;66:218–26.

[24] Parada C, Chai Y. Mandible and Tongue Development. Curr Top Dev Biol 2015;115:31–58.

[25] Messina G, Biressi S, Monteverde S, Magli A, Cassano M, Perani L, et al. Nfix regulates fetal-specific transcription in developing skeletal muscle. Cell 2010;140:554–66.

[26] Piper M, Gronostajski R, Messina G. Nuclear Factor One X in Development and Disease. Trends Cell Biol 2019;29:20–30.

[27] Gronostajski RM. Roles of the NFI/CTF gene family in transcription and development. Gene 2000;249:31–45.

[28] Johanson M, Meents H, Ragge K, Buchberger A, Arnold HH, Sandmöller A. Transcriptional activation of the myogenin gene by MEF2-mediated recruitment of myf5 is inhibited by adenovirus E1A protein. Biochem Biophys Res Commun 1999;265:222–32.

[29] Funk WD, Wright WE. Cyclic amplification and selection of targets for multicomponent complexes: Myogenin interacts with factors recognizing binding sites for basic helix-loop-helix, nuclear factor 1, myocite-specific enhancer-binding factor 2, and COMP1 factor. Proc Natl Acad Sci USA 1992;89:9484–8.

[30] Driller K, Pagenstecher A, Uhl M, Omran H, Berlis A, Gründer A, Sippel AE. Nuclear factor

I X deficiency causes brain malformation and severe skeletal defects. Mol Cell Biol 2007;27:3855–67.

[31] Rossi G, Bonfanti C, Antonini S, Bastoni M, Monteverde S, Innocenzi A, et al. Silencing Nfix rescues muscular dystrophy by delaying muscle regeneration. Nat Commun 2017;8:1055. doi:10.1038/s41467-017-01098-y.

[32] Biressi S, Tagliafico E, Lamorte G, Monteverde S, Tenedini E, Roncaglia E, et al. Intrinsic phenotypic diversity of embryonic and fetal myoblasts is revealed by genome-wide gene expression analysis on purified cells. Dev Biol 2007;304:633–51.

[33] Torii D, Soeno Y, Fujita K, Sato K, Aoba T, Taya Y. Embryonic tongue morphogenesis in an organ culture model of mouse mandibular arches: blocking Sonic hedgehog signaling leads to macroglossia. In Vitro Cell Dev Biol Anim 2016;52:89–99.

[34] Kaufman MH. The Atlas of Mouse Development. 2nd ed. San Diego CA: ACADEMIC PRESS;1995.

[35] Yamane A, Mayo M, Shuler C, Crowe D, Ohnuki Y, Dalrymple K, et al. Expression of myogenic regulatory factors during the development of mouse tongue striated muscle. Arch Oral Biol 2000;45:71–8.

[36] Gagan J, Dey BK, Layer R, Yan Z, Dutta A. MicroRNA-378 targets the myogenic repressor MyoR during myoblast differentiation. J Biol Chem 2011;286:19431–8.

Figure Legends

Fig. 1. Specific interest and experimental design of this study. (A) Schematic representation of myogenic linage differentiation in limb. Myoblast differentiation markers are indicated in green. (B) Preparation of whole transcripts from mouse tongue. Excision margins are indicated by arrows; the medial part of the fused mandibular prominences at E10.5 and the emerged lingual swellings at E11.5. MxA, maxillary arch; MA, mandibular arch; LLS, lateral lingual swellings. Scale bars, 500 μm in macroscopic image and 200 μm in H-E staining. The flowchart indicates RNA sampling procedure.

Fig. 2. Morphogenesis and gene expression patterns of developing mouse tongue. (A) Hematoxylin and eosin (H–E) staining of tongue primordia in chronological order from E10.5 through E15.5. Scale bar = 250 μm. (B) Magnified views of tongue tissues corresponding to the yellow box in A. Immunostaining of desmin in each consecutive section. Positive signals were detected by DAB (brown), and nuclei were counterstained with hematoxylin. Scale bar = 50 μm. (C) Time-series expression patterns of major MRFs and muscle-related genes detected via qPCR. The relative expression level of each gene was normalized according to the lowest value, which was arbitrarily defined as 1. Error bars indicate ± SEM; ND, not detected. **P* <0.05, only the items correspond to microarray datasets (E10.5–E11.5 and E11.5–E14.5) are indicated.

Fig. 3. Expression profiles of myoblast differentiation marker genes. Time-series expression patterns of embryonic (A) and fetal (B) myoblast markers detected via qPCR. The relative expression level of each gene was normalized according to the lowest value, which was arbitrarily defined as 1. Error bars indicate ± SEM; ND, not detected. **P* <0.05, only the items correspond to microarray datasets (E10.5–E11.5 and E11.5–E14.5) are indicated.

Fig. 4. Localization of Nfix-expressing cells in mouse tongue. (A) Representation of myogenic cell population by a muscle differentiation marker desmin (green). Cell nuclei were stained with DAPI (blue). Scale bar = 100 μm. (B) Desmin-expressing cells in combination with MyoD (red; upper panels) or Nfix (red; lower panels) was detected in mouse tongue at E11.5 and E14.5 (magnified views of rectangular area in A). Cell nuclei were stained with DAPI (blue). Scale bar = 50 μm.

Fig. 5. Effects of *Nfix* inhibition on tongue myogenesis *in vitro*. (A) Histological and macroscopic appearances of E10.5-derived tongue primordia at the beginning (0 h), 48 h, and the end (96 h) of the culture period. MA, mandibular arches; T, tongue. Scale bar = 200 μm. (B) *In*

vitro-formed tongue primordium after 48 and 96 h of culture with either control (scrambled) or *Nfix*-targeted antisense oligonucleotide. H–E staining and immunostaining of Ki-67 and desmin are shown. A cell-free space emerged in the *Nfix*-inhibited specimen is indicated by arrowheads. Elongated/spindle-shaped desmin-positive cells are indicated by arrows. T, tongue. Scale bar = 100 μm.

Fig. 6. Expression of *Nfix* mRNA and protein product in the experimental condition. (A) The mRNA expression level of *Nfix* relative to that of the control is shown. Error bars indicate ± SEM. **P* <0.05. Immunostaining of desmin (green) and Nfix (red) for tongue primordia after 48 h of culture. Cell nuclei were stained with DAPI (blue). Scale bar = 50 μm. (B) Expression of *Nfix* and its downstream target genes *Nfatc4* and *Eno3*. The mRNA expression level of each gene relative to that of the control is shown. Error bars indicate ± SEM. **P* <0.05. (C) *In vitro*-formed tongue primordium. Tongue primordia collected from E11.5 embryos were cultured for 48 h with either control (scrambled) or *Nfix*-targeted antisense oligonucleotide. H–E staining and immunostaining of Ki-67 and desmin are shown. Scale bar = 100 μm.

Supplementary Fig. S1. Expression of miRNAs that contribute to myogenic signaling. (A) List of differentially expressed miRNAs (>2-fold) between E10.5 and E11.5. The 10 top-ranking miRNAs, based on microRNA microarray results, are shown. The myomiRs are indicated in bold, and the Nfix-targeting miRNA candidates are underlined. (B) Time-series expression patterns of myomiRs (B) and potential Nfix-targeting miRNAs (C) detected via qPCR (normalized by U6 snRNA). The relative expression level of each gene was normalized according to the lowest value, which was arbitrarily defined as 1. Error bars indicate ± SEM. *P <0.05, only the items correspond to microarray datasets (E10.5–E11.5 and E11.5–E14.5) are indicated.

Table 1. Muscle-related genes up-regulated (>5-fold) in mouse tongue primordia between E10.5 and E11.5.

Gene Symbol	Gene Title	Z-score[a]	FC[b]
Transcription factors			
Myog	myogenin	12.6	45.3
Myod1	myogenic differentiation 1	9.6	18.2
Meox2	mesenchyme homeobox 2	8.4	15.3
Smyd1	SET and MYND domain containing 1	10.4	11.8
Myf5	myogenic factor 5	7.5	11.3
Tcf21	transcription factor 21	7.1	8.6
Nfix	nuclear factor I/X	6.6	8.5
Msc	musculin	6.6	7.5
Meox1	mesenchyme homeobox 1	6.2	6.6
Lbx1	ladybird homeobox homolog 1 (Drosophila)	5.5	6.0
Nkx2-5	NK2 transcription factor related, locus 5 (Drosophila)	5.5	6.0
Structural genes			
Actc1	actin, alpha, cardiac muscle 1	16.0	58.4
Tnnt1	troponin T1, skeletal, slow	14.5	39.7
Acta2	actin, alpha 2, smooth muscle, aorta	17.9	30.1
Myl1	myosin, light polypeptide 1	10.5	29.5
Myh3	myosin, heavy polypeptide 3, skeletal muscle, embryonic	9.1	19.0
Ttn	titin	9.0	18.2
Tnnc2	troponin C2, fast	7.9	12.9
Mylpf	myosin light chain, phosphorylatable, fast skeletal muscle	7.9	11.1
Tnnt2	troponin T2, cardiac	10.1	10.9
Tnnc1	troponin C, cardiac/slow skeletal	7.7	10.3
Neb	nebulin	9.5	9.5
Myl4	myosin, light polypeptide 4	6.2	7.3
Myh8	myosin, heavy polypeptide 8, skeletal muscle, perinatal	8.1	6.7

[a]Only the genes with activation Z-scores >4 are listed.
[b]FC indicates the fold-change in gene expression between E10.5 and E11.5.

Transcription factors that regulate muscle formation and genes for myofiber component are listed. Notably, although they play no role in the predicted networks, muscle-related genes such as *Msc* and *Smyd1* were among the >5-fold upregulated genes. FC, fold-change of the microarray signal intensity.

Table 2. Activation status in biological processes of mouse tongue primordium predicted by IPA.

Functions Annotation	Categories associated	p-Value	Predicted Activation State (Z-score)	# of genes
E10.5 – E11.5				
Development of muscle	Embryonic Development, Organismal Development, Organ Development, Tissue Development, Skeletal&Muscular System Development&Function	3.8E-14	Increased (2.16)	26
Congenital anomaly of musculoskeletal system	Developmental Disorder, Skeletal & Muscular Disorders	1.5E-12	Increased (2.62)	30
Activation of DNA endogenous promoter	Gene Expression	4.6E-5	Increased (2.27)	27
Transcription of DNA	Gene Expression	2.9E-4	Increased (2.15)	32
Expression of DNA	Gene Expression	3.4E-4	Increased (2.32)	33
E11.5 – E14.5				
Contractility of muscle	Skeletal & Muscular System Development & Function	1.3E-10	Increased (4.05)	35
Congenital anomaly of musculoskeletal system	Developmental Disorder, Skeletal & Muscular Disorders	2.4E-9	Increased (2.82)	75
Contractility of cardiac muscle	Organ Morphology, Skeletal & Muscular System Development&Function, Cardiovascular System Development & Function	2.6E-8	Increased (3.16)	26
Formation of cellular protrusions	Cellular Assembly & Organization, Cellular Function & Maintenance, Cell Morphology	4.5E-8	Increased (2.19)	91
Differentiation of cells	Cellular Development	6.6E-8	Increased (2.20)	193

The five top-ranking annotations (P values < 0.05 and Z-scores > 2 [increased]) are shown. Annotation was provided primarily in association with categories, and the categories with common functional annotations were combined.

Table 3. Functional networks for early (E10.5–E11.5) and late (E11.5–E14.5) stages of tongue development predicted using microarray data.

ID	Top Functions	Molecules in Network	Score
< E10.5 to E11.5 >			
1	Embryonic Development, Organ Development, Connective Tissue Development & Function	**MEF2**,**MEOX1**,**MEOX2**,**MYOD1**,**MYOG**,**NKX2-5**,**TCF21**,*DLX2*,*DLX5*,*LIN28A*,*MSX1*,*MSX2*,*TBX2*,Alp,CDH15,CHRNG,DKK1,DLX1,EBF1,ENPP1,FNDC5,FRZB,Hdac,IRX3,MYBPC1,NFkB_(complex),OGN,OSR1,Rb,RSPO1,TNNC2,Wnt	56
2	Skeletal & Muscular Disorders, Developmental Disorder, Hereditary Disorder	**MYF5**,**NFIX**,ACTA1,ARHGAP6,CAP2,COBL,DNER,ERK1/2,FIGF,FLNC,FSH,GActin,GTPase,HMP19,JAM2,Lh,LOX,LRRN1,Myosin,NFIA,NTN1,Nuclear_factor_1,PTPRZ1,RGS4,RGS5,RGS16,Tni,TNNC1,TNNT1,TNNT2,TPM2,Tropomyosin,Troponin_t	43
3	Hereditary Disorder, Hematological Disease, Cancer	**LBX1**,ATP2A1,ATPase,CA3,CELF2,CXCL14,estrogen_receptor,IgG1,IgG,IL4,IL12_(complex),Insulin,Interferon_alpha,Jnk,Mapk,MYH3,MYH6,Neb,Nos,P38_MAPK,Pro-inflammatory Cytokine,SLN,Sos,trypsin	29
< E11.5 to E14.5 >			
1	Embryonic Development, Organismal Development, Cancer	14-3-3,AQR,BCLAF1,BZW1,Calmodulin,CCAR1,CDC5L,DEPTOR,EPB41L2,EXO1,FAM107B,FBXW11,FHL1,GBF1,IMMT,KIAA0907,MYBPC1,NPAS2,NPNT,OPCML,OSR1,**PAX7**,PDE4DIP,PLAGL1,PPIG,RAB40B,RRAD,RRM1,RRP1,SPTBN1,SRRM2,SYNPO2,WNK1,YWHAG,ZNF207	46
2	Dermatological Diseases & Conditions, Gastrointestinal Disease, Organismal Injury & Abnormalities	APOBEC2,ASPM,ASPN,BCAS2,C11orf82,CCNL2,CEP55,COL14A1,COL2A1,COL6A1,COL6A2,COL9A1,Collagen_type_VI,COP_I,CSTF1,DCK,DCN,DRAM1,FMO1,Fxyd3,GATM,HJURP,IGF2BP1,LPP,LUM,MIS18BP1,MLL5,PDLIM5,SCN3B,SGPL1,SPAG5,TP53,Ube3,WDR33,ZNF292	40
3	Cardiovascular Disease, Embryonic Development, Organ Development	ACTN2,ANKRD1,AP-3,AP3M1,B3GNT9,CAPN3,CAPN6,CSRP3,DCLK1,DLEU7,FAM46A,Filamin,HDLBP,LDB2,LDB3,LMO7,LUC7L3,MYOZ2,MYPN,NFkB_(complex),Pdlim3,PRPH,PTPLAD1,RAB31,RNF14,SERINC3,SLC8A1,SORBS2,Spectrin,STOM,TTN,VPS41,ZFAND5	38

The three top-ranked networks obtained from each of the two comparisons (E10.5–E11.5 for the early stage and E11.5–E14.5 for the late stage of tongue development) are listed. Muscle-related transcription factors are underlined, upregulated (>5-fold) genes are indicated in bold, and downregulated (>5-fold) genes are indicated in italics.

Supplementary Table S1. PCR primer sets used in this study.

Gene	Forward	Reverse
Eno3	CACTGTCCCAGCTGCTACCTA	GAGCTGGAAAGCCTTCCTTGG
Mck	TGACATCGTCCAGAGTGAAGC	ATCACATGGCCAAGGTGC
Mef2c	TGCAATCTCACAGTCGCACA	TGGATGAGCGTAACAGACAGG
Meox1	TGGGTGGGTCCAAGGTAGGACA	ACGCTGACTATCGGGCACGGAG
Meox2	TTCCACTTGAGCTGTGCTCAG	TATTCAGGAGGCCTTTCTGCC
Mrf4	GATGCAGGAGCTGGGCGTGG	AGGTGCGCAGGAAATCCGCA
Myf5	CTTGGTTGACCTTCTTCAGGC	TTGCAAGAGGAAGTCCACTACC
Myh3	CGGAGGAGCTGTTAGCTACG	CATCACAGCCCCTGTCAGTT
Myh7	TGACGTCACCTCCAACATGG	TTGCTCCGGTGCTCATTCAT
Myh8	ATGGAGGGAGACCTGAACGA	AAACTTTCAGCAGCCAAGCG
Myod1	AGACCTTCGATGTAGCGGATG	AGTGAATGAGGCCTTCGAGAC
Myog	ACACCCAGCCTGACAGACAAT	TACGTCCATCGTGGACAGCAT
Nfatc4	CGGATTACTGGCAAGATGGT	TTCTCTGGGAGCAAGGTCAT
Nfix	GTGACCCTGGGAAGGCGGTCC	CCCTGCATCCACGTCATTGGGCCA
Pax3	TGCGTTCGAAGGAATAGTGCT	TCTATTCCACAAGCCGTGTCA

Fig. 1

A

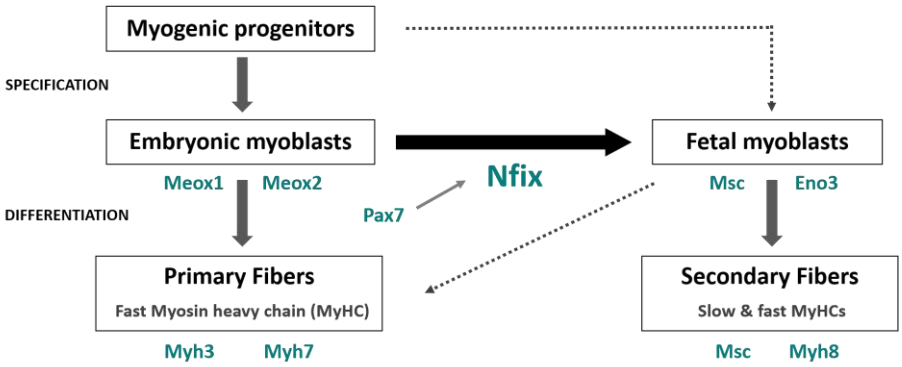
Myogenic progenitors
SPECIFICATION
Embryonic myoblasts
Meox1
Meox2
DIFFERENTIATION
Pax7
Nfix
Fetal myoblasts
Msc
Eno3
Primary Fibers
Fast Myosin heavy chain (MyHC)
Myh3
Myh7
Secondary Fibers
Slow & fast MyHCs
Msc
Myh8

B

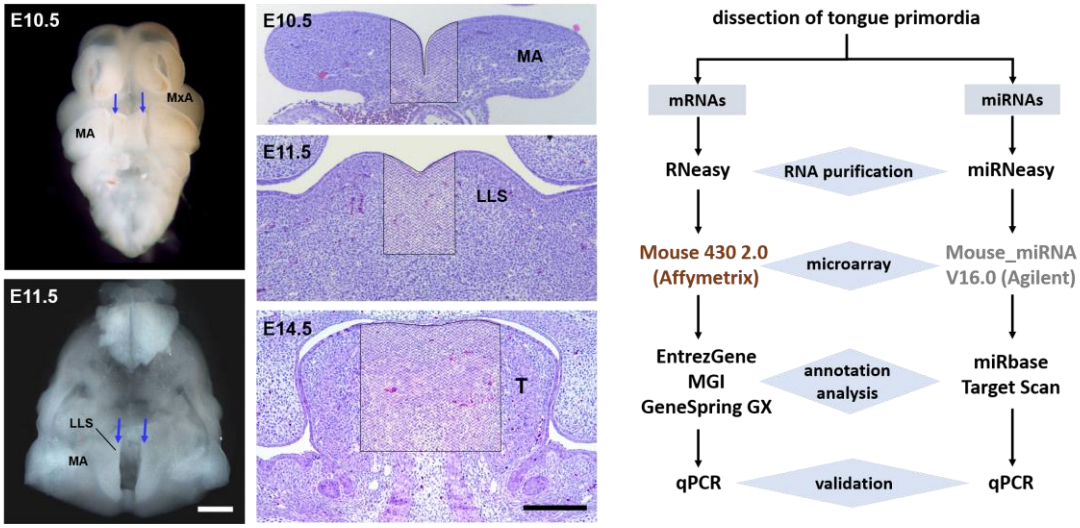
E10.5
MxA
MA
E11.5
LLS
MA
E10.5
MA
E11.5
LLS
E14.5
T
dissection of tongue primordia
mRNAs
miRNAs
RNeasy
RNA purification
miRNeasy
Mouse 430 2.0 (Affymetrix)
microarray
Mouse_miRNA V16.0 (Agilent)
EntrezGene MGI GeneSpring GX
annotation analysis
miRbase Target Scan
qPCR
validation
qPCR

Fig. 2

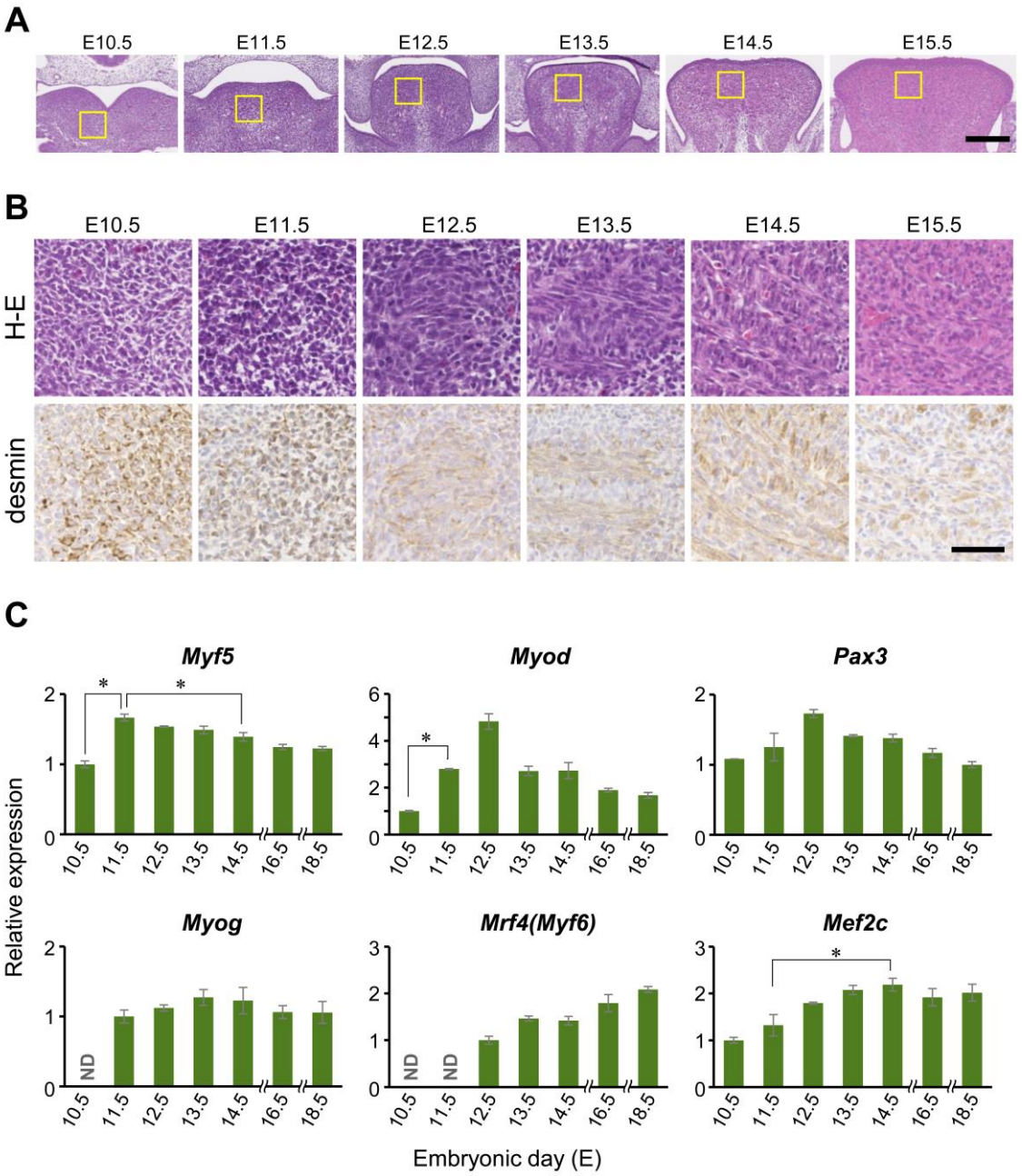
A
E10.5
E11.5
E12.5
E13.5
E14.5
E15.5
B
E10.5
E11.5
E12.5
E13.5
E14.5
E15.5
H-E
desmin
C
Myf5
Myod
Pax3
Myog
Mrf4(Myf6)
Mef2c
Relative expression
ND
10.5
11.5
12.5
13.5
14.5
16.5
18.5
Embryonic day (E)

Fig. 3

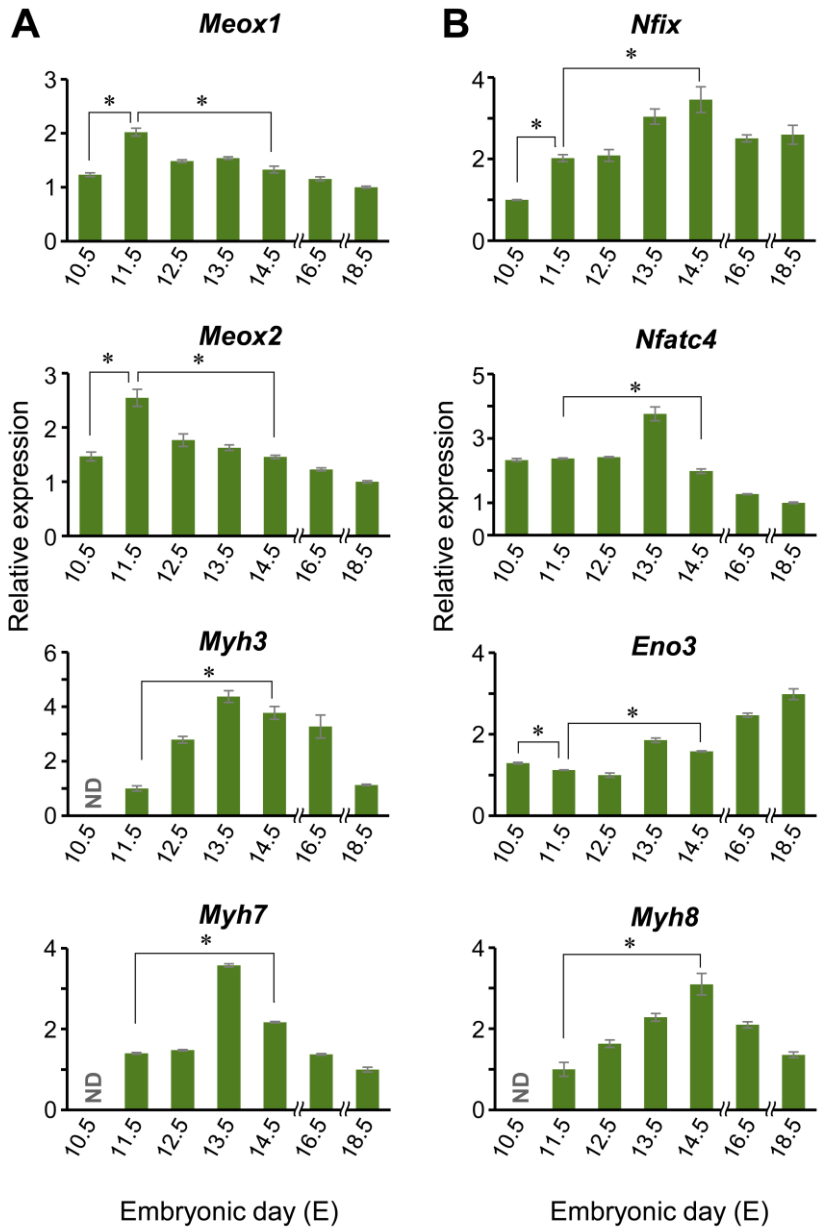
A
Meox1
Meox2
Myh3
Myh7
B
Nfix
Nfatc4
Eno3
Myh8
Relative expression
ND
10.5
11.5
12.5
13.5
14.5
16.5
18.5
Embryonic day (E)

Fig. 4

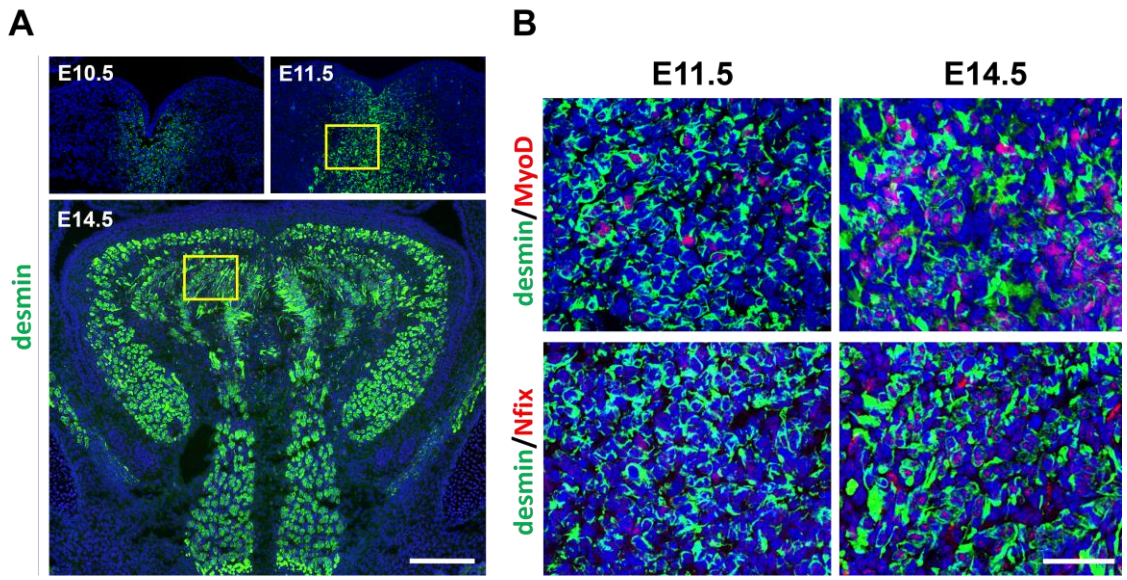

Fig. 5

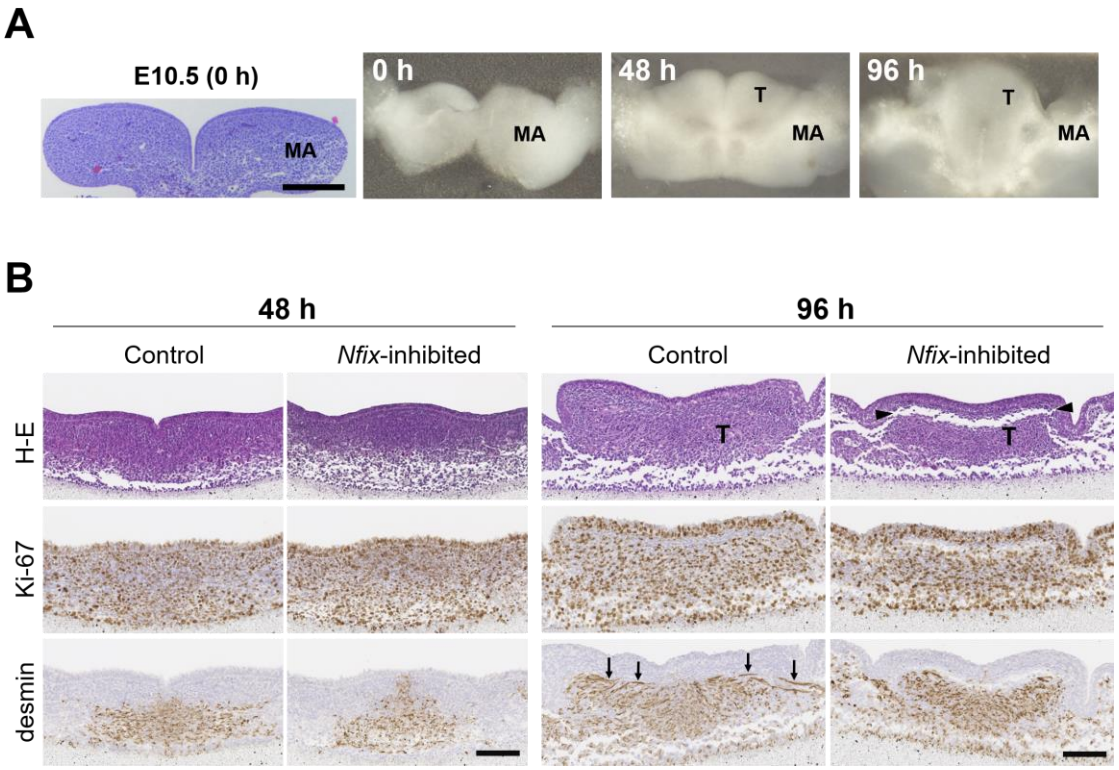
A
E10.5 (0 h)
MA
0 h
MA
48 h
T
MA
96 h
T
MA
B
48 h
96 h
Control
Nfix-inhibited
Control
Nfix-inhibited
H-E
Ki-67
desmin
T
T

Fig. 6

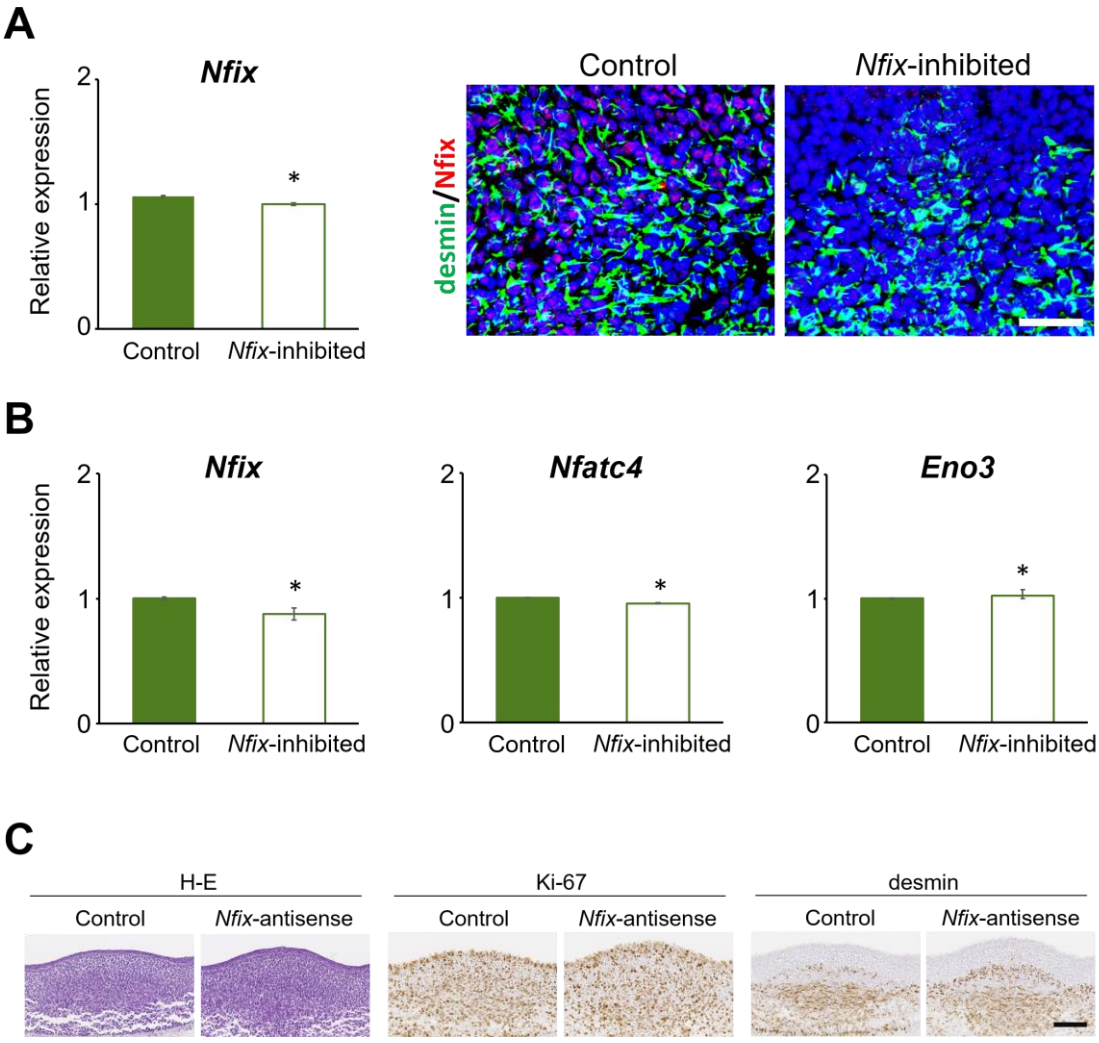
A
Nfix
Relative expression
2
1
0
*
Control
Nfix-inhibited
Control
Nfix-inhibited
desmin/Nfix
B
Nfix
Nfatc4
Eno3
Relative expression
2
1
0
*
Control
Nfix-inhibited
C
H-E
Ki-67
desmin
Control
Nfix-antisense

Supplementary Fig. S1

A

miRNA	Ratio
miR-206	*8.4E+2*
miR-133b	*6.0E+2*
miR-378	*3.5E+2*
miR-1	*2.7E+2*
miR-152	*2.5E+2*
miR-143	*2.3E+2*
miR-210	*2.1E+2*
let-7b	*2.0E+2*
miR-3099	*1.9E+2*
miR-1927	*1.9E+2*

B

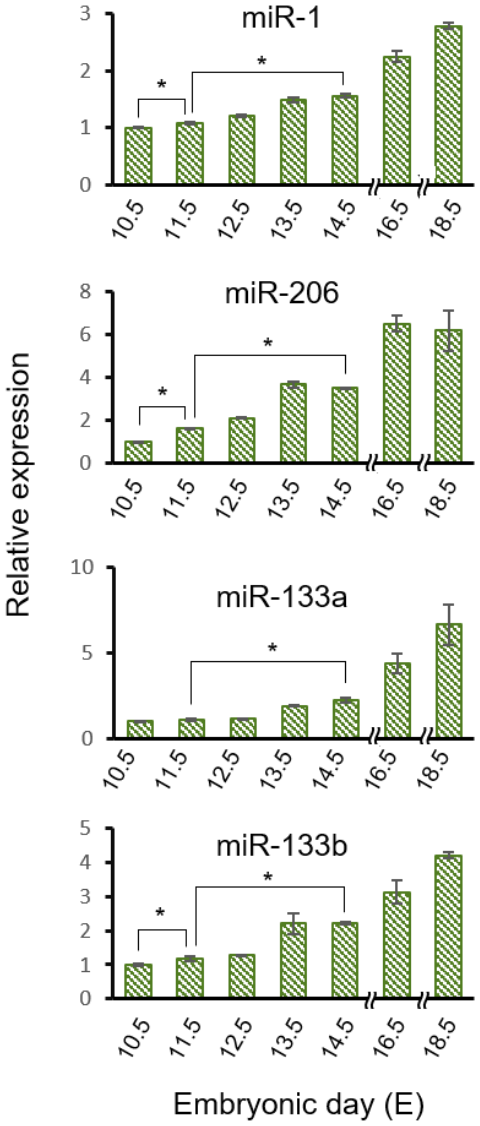

C